

Spring 2018

High Fidelity Conceptual Design of a Supersonic Aircraft

Daniel Donahue

Washington University in St. Louis, dangdonahue@yahoo.com

Follow this and additional works at: <https://openscholarship.wustl.edu/mems5001>

Recommended Citation

Donahue, Daniel, "High Fidelity Conceptual Design of a Supersonic Aircraft" (2018). *Optimization Methods in Engineering*. 2.
<https://openscholarship.wustl.edu/mems5001/2>

This Article is brought to you for free and open access by the Mechanical Engineering & Materials Science at Washington University Open Scholarship. It has been accepted for inclusion in Optimization Methods in Engineering by an authorized administrator of Washington University Open Scholarship. For more information, please contact digital@wumail.wustl.edu.

High Fidelity Conceptual Design of a Supersonic Aircraft

Daniel G. Donahue

Washington University in St. Louis, April 2018

Abstract:

This paper discusses a method to find an optimum design for a supersonic aircraft. The problem approached was optimizing the Lift-to-Drag ratio of an aircraft travelling at supersonic speeds. This was done through the use of Computer Aided Design (CAD) and Computational Fluid Dynamic (CFD) software. By setting up an initial model and allowing for several of the dimensions to be variable, a variety of aircraft shapes could be made to represent different design models. These models represented a population that could be optimized using a genetic algorithm. This paper utilized a Particle Swarm Optimization scheme, which led the population towards a converged solution. Stopping criteria was established to provide a stopping point for the population evolution and was met after four iterations.

Introduction:

A need for a high fidelity conceptual design process is ever growing in the aerospace engineering industry. The faster a design can go from paper, to a feasible and useful concept, the less the overall project will cost. Faster production of a feasible design also allows for more analysis by engineers to ensure the aircraft is safer and more reliable. Being able to optimize this early portion of the design process would enable engineers to perform more analysis on a preliminary design by attaining a feasible conceptual design in a timely manner.

Historically conceptual design has been done by the way of pen and paper. By using free body diagrams and historical efficiency and sizing factors, engineers have been able to design planes that are still flying today. Advances in computational power have been able to improve the conceptual design process through the use of source panel and vortex lattice models to get an idea of aircraft performance. Newer design methods include the use of CAD and CFD software. By generating three-dimensional models and analyzing the flow around them, engineers can extract the aerodynamic coefficients and determine the performance of

the aircraft. By determining an optimum design quickly, a program can reduce conceptual design costs and focus on the safety and reliability of the production aircraft.

This paper discusses a particle swarm optimization scheme to find an optimum aerodynamic solution. Particle swarm optimization is a type of genetic algorithm that begins with an initial generation and then creates a new generation that is guided by the best value of a fitness function. The scheme developed for this paper is outlined in the Model Summary section and an example of the optimization scheme in work is provided in the Results section.

Background/Related Work:

The idea behind this paper and problem came from a research project that the author worked during undergraduate studies at Iowa State University. This research addressed a similar task of designing a transportation aircraft and pulled from different areas of multi-disciplinary analysis and optimization methodologies. One of the students who collaborated on that research project went on to

write their Master's thesis on the subject (Watson).

Other areas of engineering design optimization have called for the use of CAD and CFD software in combination. However, the majority of these studies have been on a component-based scale (IndiaCADworks). Setting up simulations and creating the correct geometry takes a lot of computational time and therefore it is typically limited to only optimizing an airfoil or wing at most. The scope of this paper was to address the macroscopic concept of optimizing for the entire platform. Namely, optimizing the shape of an aircraft for peak performance. Some recent research has looked into this macroscopic view while utilizing both CAD and CFD software but admits that it is limiting the results by ignoring some of the viscous effects that should be present in the flow field simulations (Ronzheimer). This reduces the fidelity of the optimized design, something that this paper wishes to address by studying a high-fidelity conceptual design process.

Model Summary:

The problem discussed is contained within a highly non-linear, continuous design space that is a function of the aircraft geometry. In order to put a bound on the scope of the design space, only eight parameters were allowed to be variable within the design and are outlined below. The design space can be considered highly non-linear as the aerodynamic interactions around the model are not easily predicted without running multiple turbulent based CFD cases, which was done for this paper. However, it can be assumed that the design space is continuous as there must be continuous geometry that defines the three-dimensional aircraft. As this problem contains a large design space, the particle swarm optimization scheme developed is considered to be heuristic, and a

near-local maximum can be determined at best. No global optimum for the fitness function can be obtained with this method due to the complexity of the problem.

To conduct the particle swarm optimization analysis, an initial three-dimensional model was created in the SolidWorks CAD software. After completing a baseline design, a Design Table was created and used to map eight variable dimensions to the aircraft model. Four of these variables were mapped to the Wing and four were mapped to the V-Tail. These became the eight design variables used during the optimization process. Each of the design variables were allowed to vary between maximum and minimum values.

Variables used to describe the Wing:

Root Chord Length (in): $360 \leq x_1 \leq 480$

Tip Chord Length (in): $120 \leq x_2 \leq 360$

Span (in): $360 \leq x_3 \leq 720$

Quarter Chord Sweep (deg): $80 \leq x_4 \leq 110$

Variables used to describe the V-Tail:

Tail Dihedral (deg): $20 \leq x_5 \leq 50$

Chord Length (in): $120 \leq x_6 \leq 240$

Span (in): $120 \leq x_7 \leq 240$

Leading Edge Sweep (deg): $90 \leq x_8 \leq 120$

The SolidWorks Design Table was then used to create ten models using the Excel RAND() function. Using this function (1), each of the eight design variables could have a random value that fell between each their respective minimum and maximum bounds. Renderings of the aircraft model are shown below for the minimum and maximum bounds. The first rendering showing a model with all of the minimum inputs and the

second rendering showing a model with all of the maximum inputs.

$$x_{i,n,0} = x_{i,MIN} + \xi(x_{i,MAX} - x_{i,MIN})$$

where $\xi = RAND(0,1)$ from Excel (1)

$x_{i,n,m}$ = Design Variable; with i indicating variable number, n indicating model number and m indicating generation number

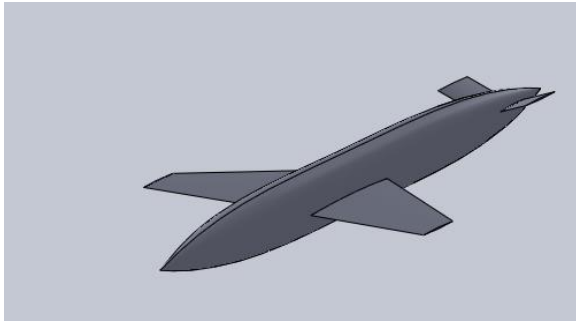


Figure 1: Renderings of Minimum Bounds on Design Variables

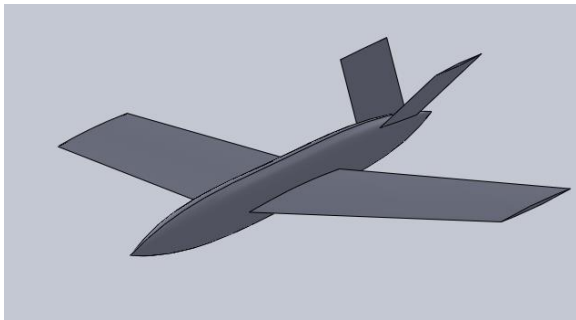


Figure 2: Renderings of Maximum Bounds on Design Variables

These initial ten models were used as the first population, referred to as Gen0 or Generation 0 and tabulated in Appendix A. The initial population was exported from SolidWorks in a Parasolid Binary format (*.x_t) and loaded into the ANSYS Fluent CFD software. Each model was then evaluated at three different angles of attack; 0 degrees, 4 degrees, and 8 degrees. All evaluations were done with a Spalar-Almaras, Turbulent Transition SST, $k - \omega$ solver at 1.5

Mach number and assumed 45kft altitude. Output for each angle of attack (α) included Axial Force (A), Normal Force (N), and in some cases Pitching Moment. This pitching moment was dropped in the later generations to save time as it was not used in the scope of this paper. Each CFD output was tabulated in an Excel worksheet and used a transformation to determine the Lift and Drag forces on the model,

$$L = N * \cos(\alpha) - A * \sin(\alpha) \quad (2)$$

$$D = N * \sin(\alpha) + A * \cos(\alpha) \quad (3)$$

Realizing that Drag can be modeled as a second order polynomial of Lift, the Lift-to-Drag ratio could then be modeled as such,

$$\frac{L}{D} = c_1\alpha^2 + c_2\alpha + c_3 \quad (4)$$

Which could then be evaluated to find a maximum Lift-to-Drag ratio for each model.

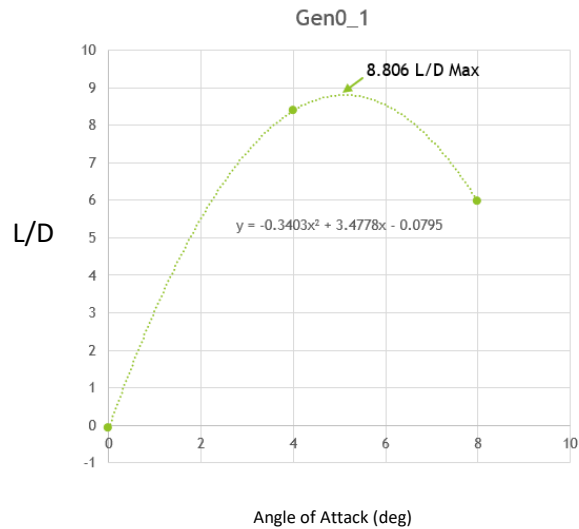


Figure 3: Graph Showing Second Order Approximation for L/D

Once each model had been evaluated in the generation, the maximum of all models was determined and set the best design for that generation. Finding the maximum Lift-to-Drag ratio for the generation was the fitness function for the optimization scheme,

$$F_{b,m} = \text{Max} \left(\left(\frac{L}{D} \right)_{MAX} \text{ of } D_{n,m} \right) \rightarrow x_{i,b,m} \quad (5)$$

where $D_{n,m}$ represents model n in generation m and $F_{b,m}$

indicates the best design from generation m and determines the best design variables, $x_{i,b,m}$, for that generation

The best design variables, $x_{i,b,m}$, from the previous generation were then used to advance the design variables for the next generation through the Design Table,

$$x_{i,n,m+1} = x_{i,n,m} + 1.1\xi(x_{i,b,m} - x_{i,n,m}) \quad (6)$$

A factor of 1.1 was applied to the advancement function (6) to allow for mutations that could bring future generations past the previous best designs' variables. Once the next generation's design variables were determined, the process was repeated to determine the next best Lift-to-Drag ratio. This process became the particle swarm optimization method used to advance towards an optimum solution. To determine if an optimum solution had been found, stopping criteria was set with,

$$\epsilon = \frac{L/D_{Max} - L/D_{Avg}}{L/D_{Max}} \leq 0.01 \quad (7)$$

This stopping criterion shows convergence towards an optimum solution by setting a small error between a generations' maximum and average Lift-to-Drag ratio.

Results:

In total, four generations were evaluated. This included the initial Gen0 and three following generations. The fourth generation, Gen3, met the stopping criteria of $\epsilon = 0.006 \leq 0.01$ and therefore the iterations commenced. As the generations evolved, the average Lift-to-Drag maximum increased for the population. This was an expected result from the particle swarm optimization method chosen. The overall maximum Lift-to-Drag was held constant for the first three generations, which was a product of the initial generation containing a random model near the optimum Lift-to-Drag ratio. Results from each generation are tabulated in Table 1 and plotted in Figure 4. Individual results are tabulated in Appendix B. As mentioned before, the optimum found is not considered to be a local or global maximum, but rather a near-local maximum for the fitness function of the particle swarm optimization.

	Gen0	Gen1	Gen2	Gen3
Gen	0	1	2	3
avg	8.45	8.84	8.93	8.98
best	9.02	9.02	9.02	9.04
delta	0.58	0.19	0.10	0.06
SC	0.064	0.021	0.011	0.006
worst	7.59	8.66	8.83	8.88

Table 1: Generation Results

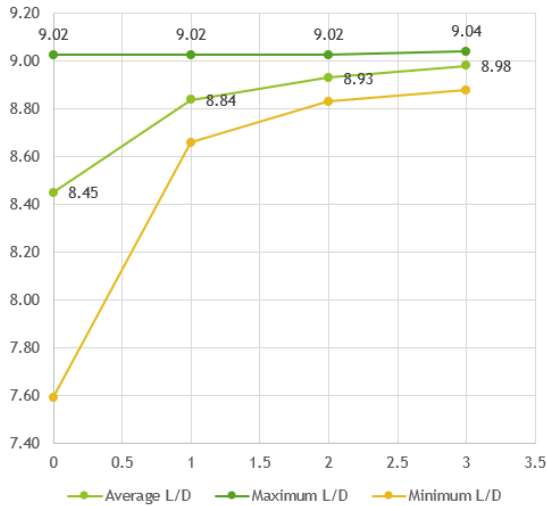


Figure 4: Graph Showing Generational Advancement to Optimum Solution

Data collection proved to be a laborious task for this problem. In total, around 384 processor-hours were required to run all of the CFD cases. This was done by utilizing 8 computers in one of the computer labs in Washington University for 8 hours straight. The geometry updates were very quick once the CFD data had been collected and therefore isn't accounted for in the above time estimate. Ways to combat this are detailed in the Continuing Work section.

In conclusion, a particle swarm optimization scheme was developed and used to

optimize aircraft performance for a supersonic transportation vehicle. Although the results used an abundance of computational power, the scheme worked as desired and showed that optimization methods could be used to determine a high-fidelity conceptual design.

Continuing Work:

If a more optimum solution were desired, the generation population sizes could be increased to allow for more data points. Also, the convergence criteria could be set to a lower value, requiring more generations to converge. To do this the author suggests using automation on top of this optimization. By writing scripts to automate the CAD and CFD process, the process could be made to be hands-off.

This project could be taken a step further by including more design variables to better describe the shape of the aircraft. Different types of aircraft models could also be tested to optimize the aircraft shape. This could include different tail and wing shapes. On top of this, Finite Element Analysis (FEA) could also be used to optimize the structure even more. Through CFD the aerodynamic loads on the aircraft can be determined, FEA could then be run to see what types of materials should be used or help define the interior structure of the aircraft.

References:

- J. Watson. "A high-fidelity approach to conceptual design". Iowa State University Digital Repository. 2016. <https://lib.dr.iastate.edu/cgi/viewcontent.cgi?article=6190&context=etd>
- IndiaCADworks. "The Use of CAD, FEA, and CFD in Engineering Design Optimization". March 25, 2015. <https://www.indiacadworks.com/blog/the-use-of-cad-fea-and-cfd-in-engineering-design-optimization/>
- A. Ronzheimer. "CFD in Aerodynamic Aircraft Design". DLR, Institute of Aerodynamics and Flow Technology. Braunschweig, Germany. 2017. http://elib.dlr.de/117320/1/PaperDGLRK2017_1_asmods.pdf

Appendix A:

This Appendix A contains the SolidWorks Design Tables for each generation along with renderings for each of the models within the population. A star is provided on the renderings to show which model had the highest lift-to-drag ratio.

Design Table for: Aspen1_dt		Wing				V-Tail			
		Root Chord	Tip Chord	Span	Sweep	Dyhdral	Chord	Span	Sweep
Design Table for: Aspen1_dt		D1@Wing_Geom	D4@Wing_Geom	D5@Wing_Geom	D2@Wing_Geom	D2@Tail_angle	D1@Tail_Geom	D4@Tail_Geom	D3@Tail_Geom
Min		360	120	360	80	20	120	120	90
Max		480	360	720	110	50	240	240	120
Gen0_1		383.3641655	311.2352916	643.3681747	103.7550373	21.7297199	193.11545	239.681753	103.151154
Gen0_2		378.2589251	294.4228634	583.5427234	83.96347489	48.3939989	207.380447	132.888062	119.596736
Gen0_3		366.3987978	346.2152122	635.4462859	95.79491601	31.2132357	183.604702	232.976058	99.5534841
Gen0_4		416.3810985	201.5645505	709.8877117	87.12693445	26.5157716	148.821142	213.245368	100.393851
Gen0_5		452.1760289	160.8383813	402.2807379	97.7875532	32.2265686	153.585869	156.861106	119.512997
Gen0_6		448.7013415	317.8283413	645.0557777	88.06074352	39.63755	159.98841	122.94461	111.49888
Gen0_7		369.3597995	252.8247242	527.3538773	92.11443351	37.2549848	217.128374	167.855157	113.38014
Gen0_8		412.4099154	215.9824468	444.9748747	94.37946679	45.9012823	141.911298	128.651627	118.98242
Gen0_9		418.2330633	287.7442782	489.7644319	100.9626259	28.0629467	209.381603	215.542027	117.847551
Gen0_10		419.7280954	263.4774474	599.2867225	85.55592524	21.4180667	196.315211	151.205786	97.8709389

Table 2: Design Table for Generation 0

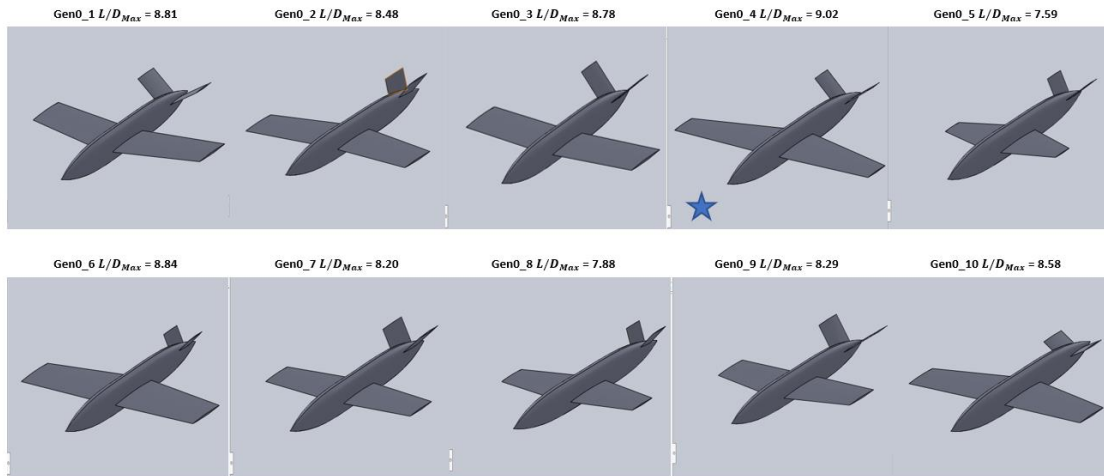


Figure 5: Renderings of Generation 0 with Maximum Lift-to-Drag Ratio for Each Model

Design Table for: Aspen1_dt			Wing				V-Tail			
			Root Chord	Tip Chord	Span	Sweep	Dyhedral	Chord	Span	Sweep
Design Table for: Aspen1_dt										
			D1@Wing_Geom	D2@Wing_Geom	D3@Wing_Geom	D3@Wing_Geom	D1@Tail_angle	D1@Tail_Geom	D4@Tail_Geom	D3@Tail_Geom
Min			360	120	360	80	20	120	120	90
Max			480	360	720	110	50	240	240	120
Gen1_1			412.9463379	296.9828771	684.8056858	97.46055073	23.3022948	164.707413	227.326909	102.567316
Gen1_2			389.7123651	195.7494033	659.5195269	85.25754568	30.1097435	183.387818	191.596576	113.497446
Gen1_3			367.7242363	305.7251487	683.2257446	92.24901468	29.9077836	153.65038	226.99234	100.080919
Gen1_4			416.3810985	201.5645505	709.8877117	87.12693445	26.5157716	148.821142	213.245368	100.393851
Gen1_5			418.7694138	162.0377339	638.1596959	89.92161364	30.9987016	153.089615	198.939258	118.326641
Gen1_6			420.1452409	228.6851259	653.4844036	87.74798266	39.1644902	150.955447	216.361574	108.429674
Gen1_7			399.896072	227.3214196	651.8896467	88.72770243	35.8501173	153.603745	207.896973	110.642885
Gen1_8			412.5224218	210.0529195	637.8874171	87.47213475	26.5534177	142.433928	164.768283	99.8553203
Gen1_9			416.3924555	218.0640058	604.4045794	93.79586023	28.0053518	150.937053	214.7663	104.672046
Gen1_10			417.670176	254.6411803	623.1879196	87.14263573	21.6072289	158.853291	215.1357	98.4044958

Table 3: Design Table for Generation 0

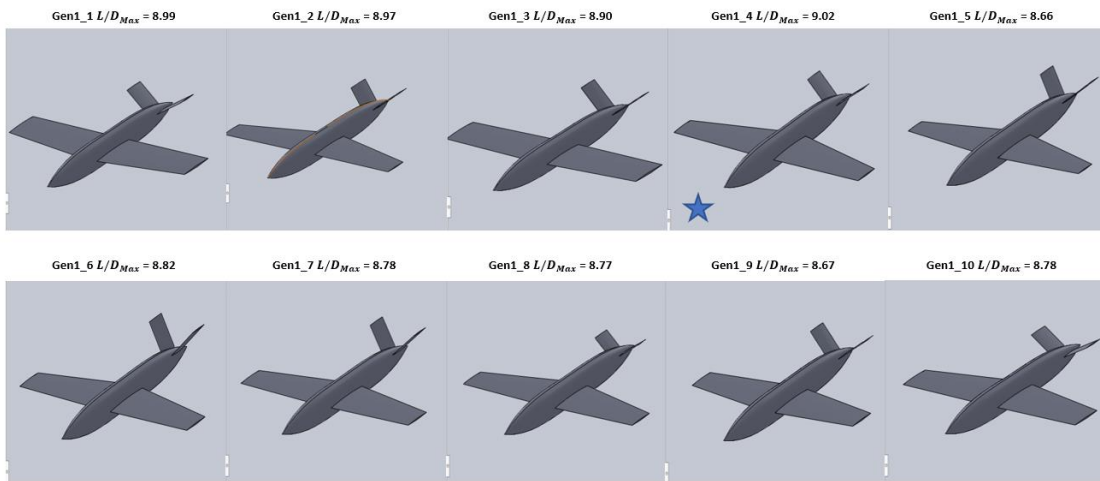


Figure 6: Renderings of Generation 1 with Maximum Lift-to-Drag Ratio for Each Model

Design Table for: Aspen1_dt		Wing				V-Tail			
		Root Chord	Tip Chord	Span	Sweep	Dihedral	Chord	Span	Sweep
Design Table for: Aspen1_dt		$D1@Wing_Geom$	$D2@Wing_Geom$	$D3@Wing_Geom$	$D3@Wing_Geom$	$D1@Tail_angle$	$D1@Tail_Geom$	$D2@Tail_Geom$	$D3@Tail_Geom$
Min		360	120	360	80	20	120	120	90
Max		480	360	720	110	50	240	240	120
Gen2_1		416.1068676	271.8856146	686.7453599	89.83382286	25.0460283	152.315655	215.99673	100.527856
Gen2_2		393.4393995	198.9002939	663.5481936	85.50259498	26.6292095	173.892388	211.789829	104.707669
Gen2_3		397.8490618	246.2474666	712.0447552	91.50335878	28.7841705	151.782226	216.447116	100.170114
Gen2_4		416.3810985	201.5645505	709.8877117	87.12693445	26.5157716	148.821142	213.245368	100.393851
Gen2_5		417.6274263	182.2201313	685.7680068	87.47621338	26.6963633	151.560966	199.597119	112.950505
Gen2_6		419.2143048	218.4275343	670.267776	87.1504861	38.1540665	149.956334	215.559874	103.251387
Gen2_7		409.508622	199.1528762	699.46599	88.37361544	32.5271729	152.969315	212.106747	109.530633
Gen2_8		414.0100058	203.2863086	678.8723711	87.18804037	26.5406223	146.251046	188.504602	99.9918284
Gen2_9		416.3832004	207.2635328	709.7698215	89.73278477	26.8793868	149.159384	213.894926	103.724704
Gen2_10		417.2416885	241.6906862	642.5024347	87.13706864	26.7088311	150.840028	214.072267	98.6734135

Table 4: Design Table for Generation 0

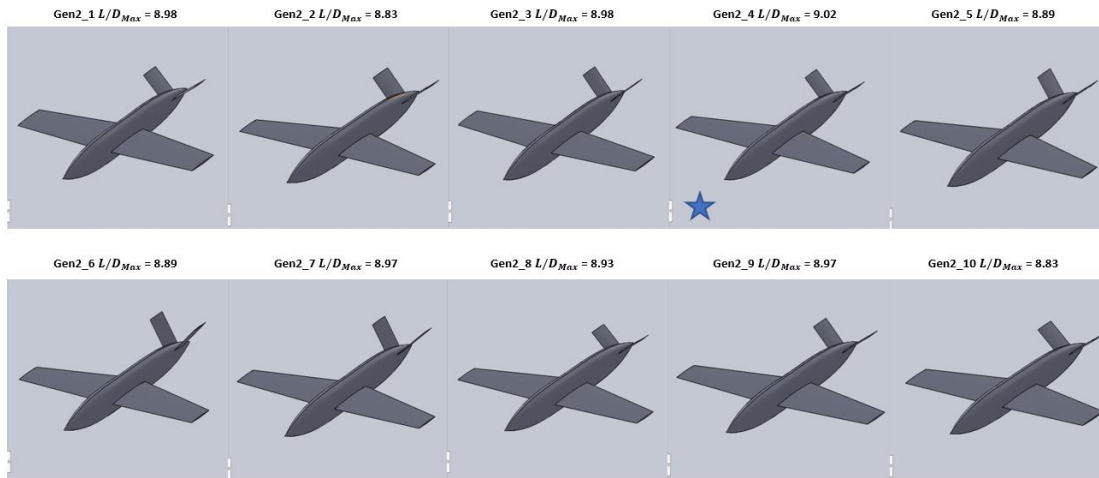


Figure 7: Renderings of Generation 2 with Maximum Lift-to-Drag Ratio for Each Model

Design Table for: Aspen1_dt_cut		Wing				V-Tail			
Design Table for: Aspen1_dt		Root Chord	Tip Chord	Span	Sweep	Dihedral	Chord	Span	Sweep
		D1@Wing_Geom	D2@Wing_Geom	D3@Wing_Geom	D4@Wing_Geom	D1@Tail_angle	D1@Tail_Geom	D4@Tail_Geom	D3@Tail_Geom
Min		360	120	360	80	20	120	120	90
Max		480	360	720	110	50	240	240	120
Gen3_1		416.4009748	242.431951	691.0607108	88.18506741	26.1554082	148.702434	213.594135	100.416779
Gen3_2		403.6631525	199.0890888	674.78437	86.27351687	26.6213945	172.928592	212.865979	100.986751
Gen3_3		410.7686004	200.5374015	710.6915908	89.44007627	28.1108927	150.750198	216.244978	100.249229
Gen3_4		416.3810985	201.5645505	709.8877117	87.12693445	26.5157716	148.821142	213.245368	100.393851
Gen3_5		416.7067008	194.4824347	707.9415729	87.47349543	26.5120419	151.490932	202.963187	100.106888
Gen3_6		416.8215712	200.6016118	689.7816385	87.13398196	38.0886701	149.060515	214.232753	102.195429
Gen3_7		410.8164642	200.8430352	704.3136889	87.74827834	29.1030755	150.461897	213.120223	105.438171
Gen3_8		415.4638549	201.8663524	698.2268589	87.16109082	26.5223687	149.02918	191.450626	100.179911
Gen3_9		416.3817619	202.7467301	709.8274483	88.3618688	26.5451419	149.145702	213.718461	101.693099
Gen3_10		416.8021673	207.892451	710.809743	87.12779533	26.6877716	150.838072	213.827609	99.7295134

Table 5: Design Table for Generation 0

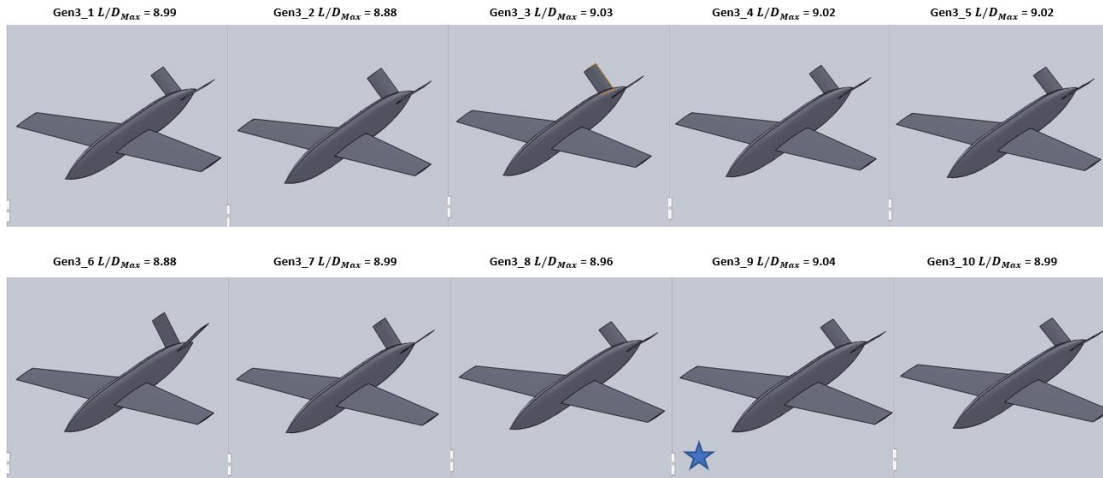


Figure 8: Renderings of Generation 3 with Maximum Lift-to-Drag Ratio for Each Model

Appendix B:

This Appendix B shows the forces output from the CFD computations. They are then converted from Normal and Axial force into Lift and Drag. Graphs are also provided with the trend lines used to calculate the maximum lift-to-drag ratio for each model.

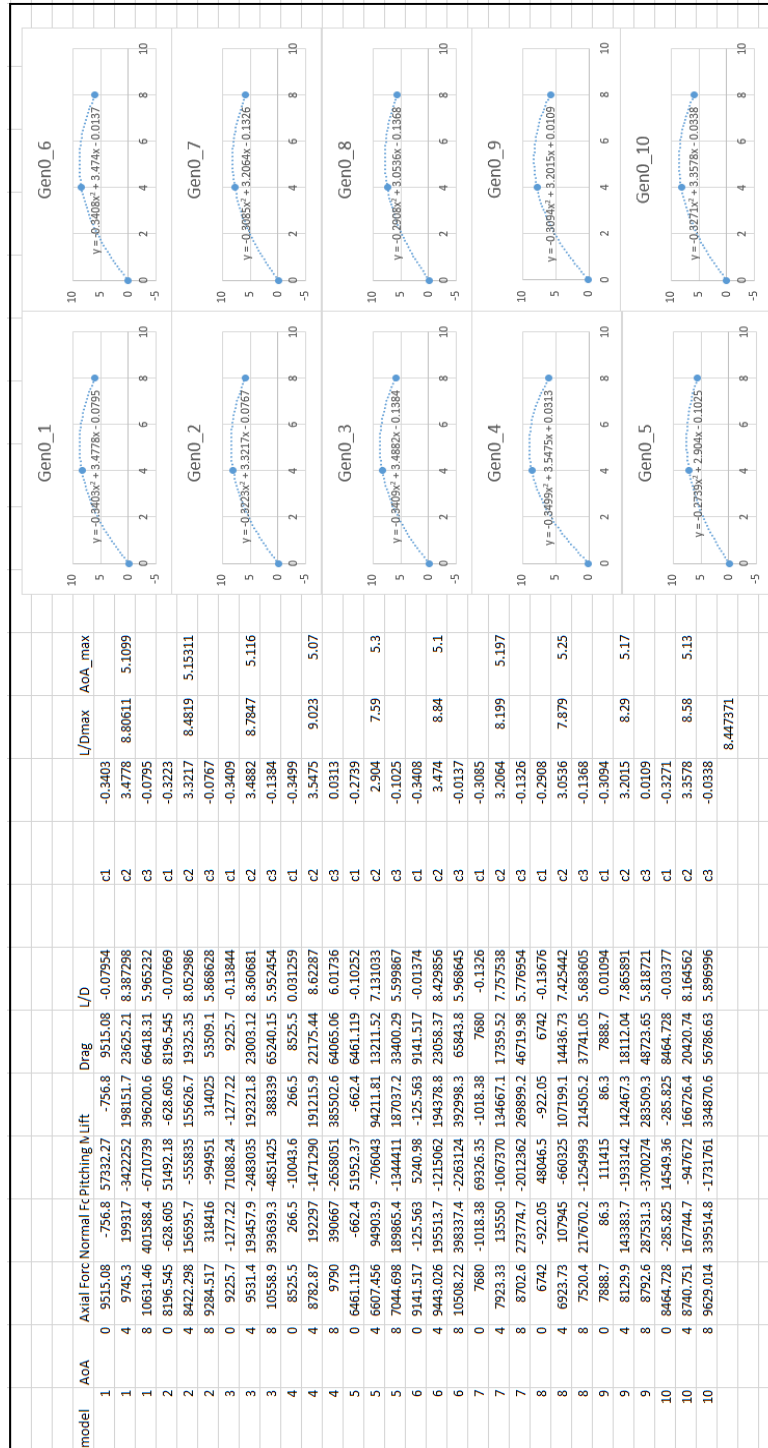


Figure 9: Generation 0 Data and Max L/D Calculation

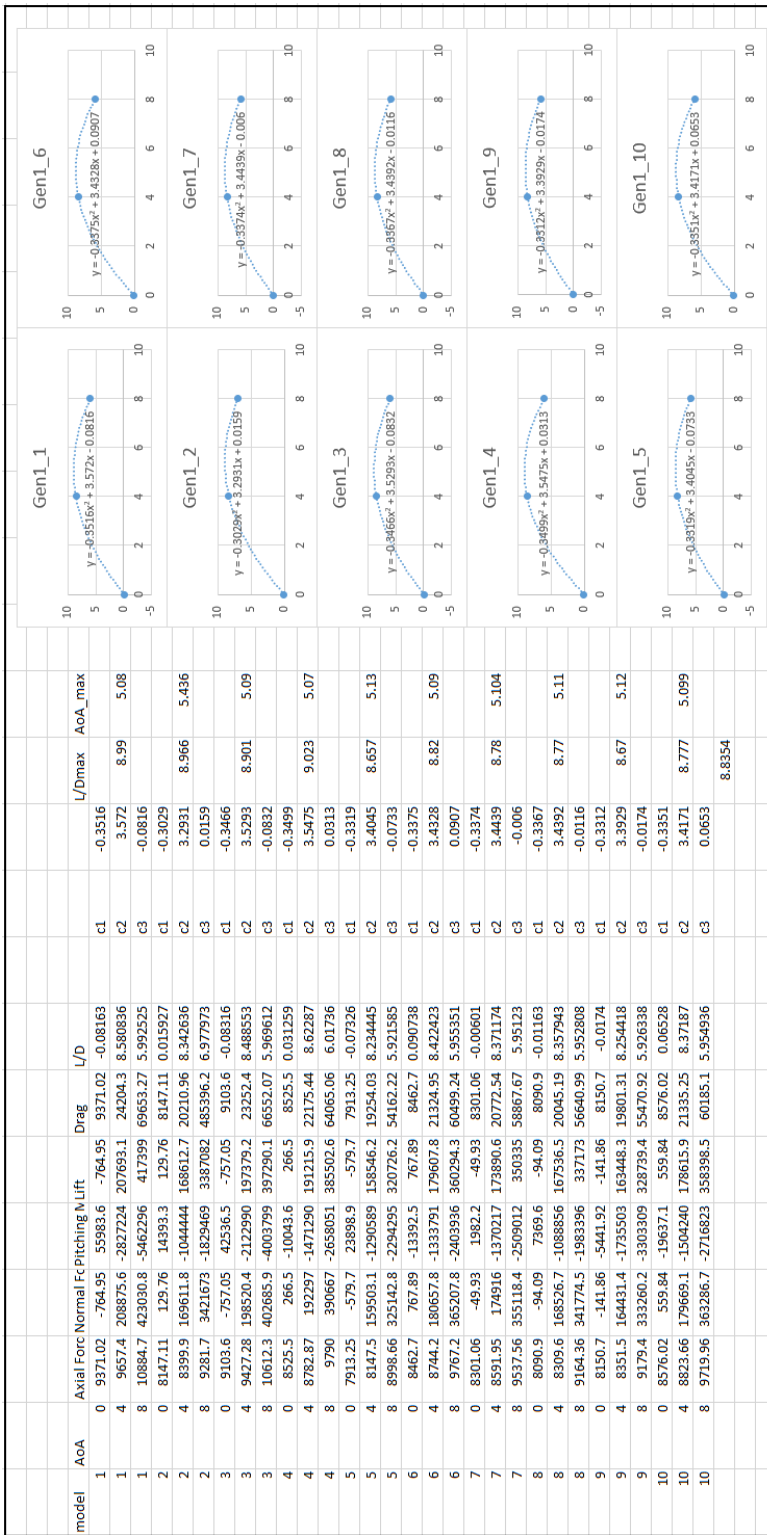


Figure 10: Generation 1 Data and Max L/D Calculation

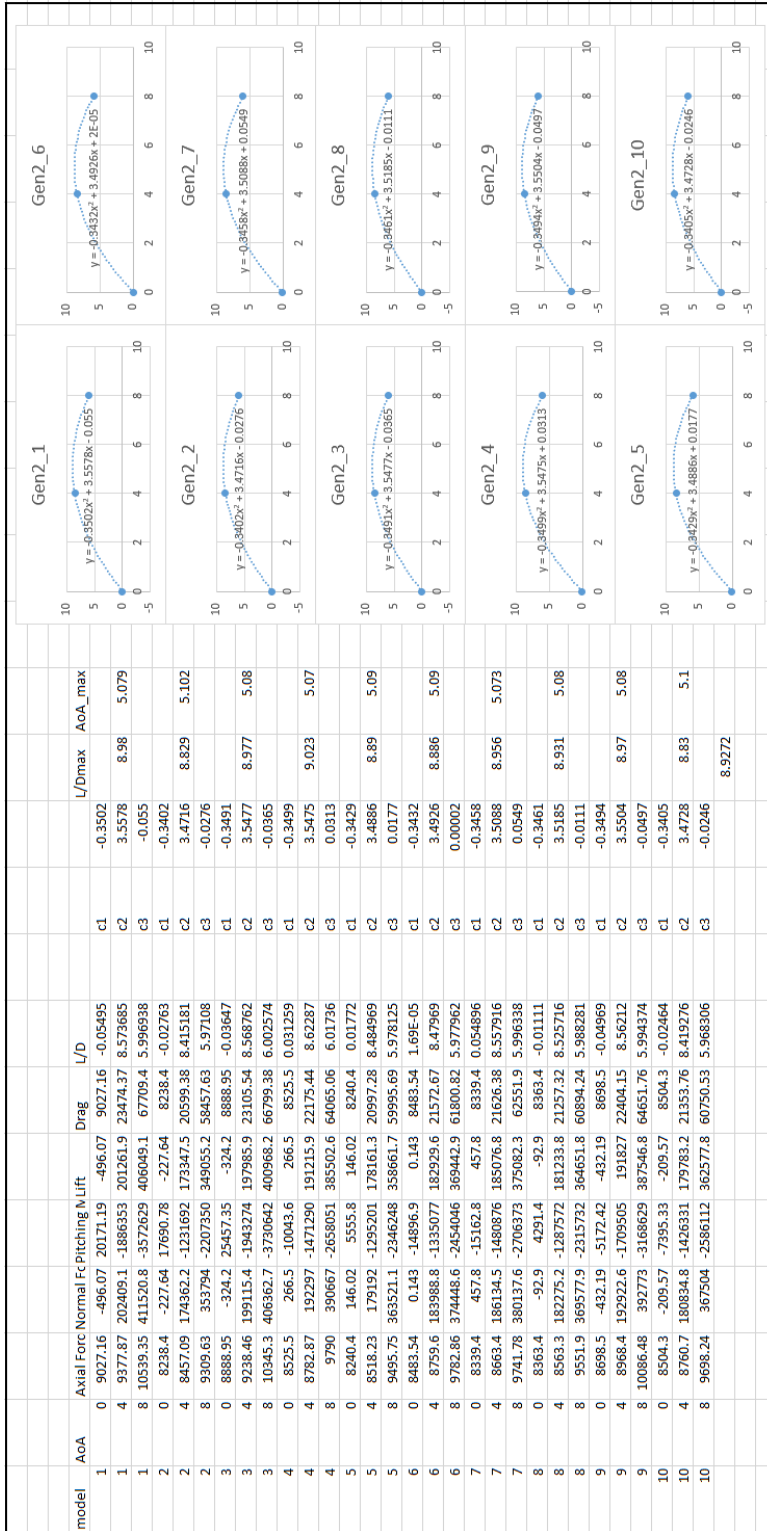


Figure 11: Generation 2 Data and Max L/D Calculation

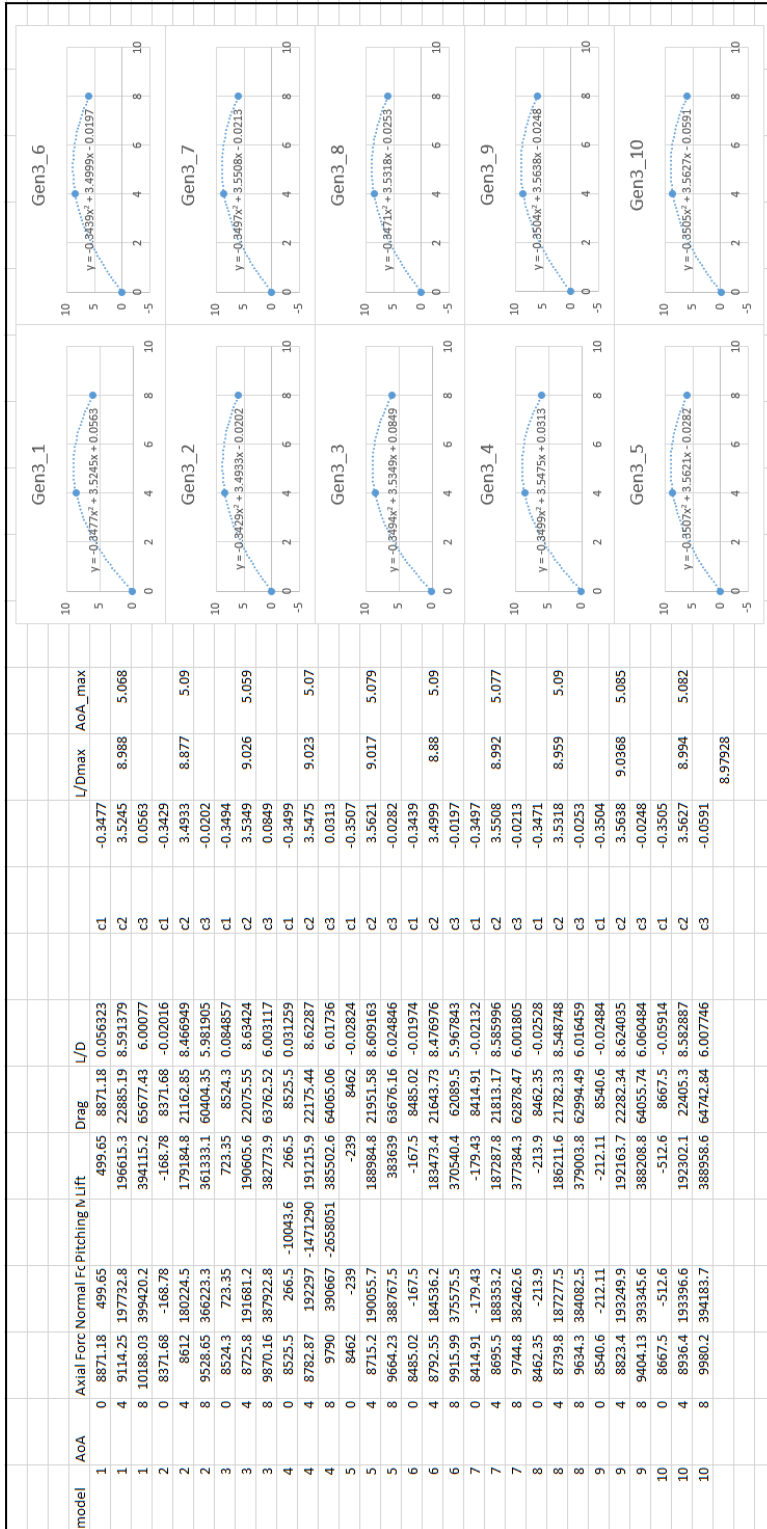


Figure 12: Generation 3 Data and Max L/D Calculation